Published in Recent Advances in Supercapacitors 4, 57-77, 2006
which should be used for any reference to this work

Structural and chemical characterization of carbons used as supercapacitors

Teresa A. Centeno[1] and Fritz Stoeckli[2]

[1]Instituto Nacional del Carbón-CSIC, Apartado 73, E-33080 Oviedo, Spain

[2]Laboratoire de Chimie Physique des Surfaces, Institut de Microtechnique de l'Université, Rue Emile Argand 11, CP 158, CH-2009 Neuchâtel, Switzerland

Abstract

This article provides a good understanding of typical activated carbons' structural and chemical properties in electrochemical capacitors, using mainly the 2 M H_2SO_4 electrolyte in the present case. Immersion calorimetry indicates that micropore systems with average widths L_o above 0.7 to 0.8 nm are equally accessible to the aqueous electrolyte and to benzene, against 0.8 to 1 nm for $(C_2H_5)_4NBF_4$ in acetonitrile. Moreover, this technique confirms that the oxygen-containing groups, which also play a role in the electrochemical properties, are distributed over the entire micropore system, and that they are not limited to the external surface area. It appears that the capacitance C (F g^{-1}) depends on both the total surface area and on the oxygen-containing surface groups, rather than on separate contributions from the microporous and external surface areas, as postulated earlier. The paper also considers correlations between the structural and the chemical properties of the carbons and the corresponding Ragone-type plots.

In the memory of late Prof. Conway

Correspondence/Reprint request: Prof. Fritz Stoeckli, Institut de Microtechnique, Université de Neuchâtel, rue Emile Argand 11, CP 158, CH-2009 Neuchâtel, Switzerland. E-mail: fritz.stoeckli@unine.ch

Introduction

Microporous carbons, and in particular activated carbons [1] are well known for their high sorptive capacities, but in recent years they have also found applications in electrical energy storage, as double-layer capacitors [2]. These applications correspond to different physical contexts, but in the last analysis surface areas, pore-size distributions and the chemistry of the surface play a fundamental role in their description. It follows that the structural and the chemical characterization of carbons, which has a great relevance in filtration technology, can also be applied to the study of carbons used as supercapacitors.

In the present paper, we wish to describe recent developments in the study of microporous carbons and to show the relevance of this approach to the description of electrochemical properties of these solids, such as the electric double layer capacitance (EDLC). Our work is based on well characterized carbons with micropore widths between 0.7 and 2 nm, thus covering the entire range of industrial materials. The electrolyte is essentially 2 M H_2SO_4, which allows a systematic study of their electrochemical properties and leads to useful correlations. The study deals with the following issues:

1. Structural aspects of activated carbons
2. Chemical groups in activated carbons and their distribution in the micropore system
3. EDLC properties of activated carbons in relation to their structural and chemical characteristics

1. Structural aspects of activated carbons

1.1. Materials and experimental details

The carbons used in the present study (Table 1) are typical materials obtained either from carbonized lignocellulosic precursors, anthracite, activated carbons black (XC-72) or petroleum pitch PX-21, which have been activated either physically (steam near 1000-1100 K) or chemically (KOH), to weight losses between 30 and 70 per cent [1]. A non-porous graphite HSAG-300, with a surface area of 335 $m^2\ g^{-1}$ was also used for comparison purposes

in electrochemistry. Table 1 shows a selection of carbons used in our laboratories [1,3-9].

All the samples were characterized by standard techniques based on vapour adsorption [1,3,4], typically with nitrogen at 77 K and/or benzene near 293-298 K, and by immersion calorimetry into liquids with various molecular dimensions [4-6]. The general theoretical framework is Dubinin's theory [1,4] with its extensions to calorimetry, and adsorption from solutions [1, 7, 8].

With the exception of KOH activated materials, industrially prepared carbons usually contain less than 1 to 1.5 mmol of surface oxygen. Therefore, in order to increase the number of surface groups and examine their effect on electrochemical properties, samples subjected to oxidation by $(NH_4)_2S_2O_8$ or nitric acid have also been considered. The amount of oxygen present on the surface can be obtained quantitatively from Thermally Programmed Desorption (TPD) [8,9], which also provides information on the type of groups generating mainly CO_2, CO, and some H_2O. For the underlying theory (Dubinin), the characterization and the experimental details, the reader is referred to reviews and specific papers [1, 3-6]. The main properties of the carbons, discussed below, are given in Table 1.

Table 1. Structural and electrochemical characteristics of a few typical activated carbons, in order of increasing L_o. Volumes W_o and surface areas S_{mi} and S_e, are averages from different techniques.

Carbon	W_o ($cm^3\ g^{-1}$)	L_o (nm)	S_{mi} ($m^2\ g^{-1}$)	S_e ($m^2\ g^{-1}$)	S_{tot} ($m^2\ g^{-1}$)	C_o ($F\ g^{-1}$)	C_o/S_{tot} ($F\ m^{-2}$)
S-3	0.26	0.70	788	6	794	125	0.157
CMS	0.25	0.75	645	20	665	115	0.173
MH2-HCl	0.49	0.9	1078	25	1103	185	0.168
XC-72-init	0.06	0.96	145	105	250	22	0.088
AZ46-0	0.33	0.96	668	140	808	136	0.168
DCG-5	0.54	1.10	982	40	1022	169	0.165
BV46	0.40	1.10	727	110	837	142	0.170
MH8HCl	0.47	1.17	804	45	849	183	0.216
PC-94-11-ox	0.48	1.18	810	20	830	156	0.188
UO2	0.45	1.26	714	105	819	128	0.156
BV46-Ox	0.42	1.29	651	112	763	155	0.203
M-30	0.70	1.33	1050	50	1100	204	0.185
Supra DLC-50	0.79	1.33	1038	11	1049	152	0.145
KF-1500	0.62	1.38	910	28	938	135	0.144
UO3	0.51	1.80	570	60	630	122	0.194
UO3-ox	0.57	1.80	630	60	690	150	0.217
PX-21	1.20	2.00	1166	104	1270	322	0.253
H25-ox	0.51	2.00	607	43	650	130	0.200
N-125	0.64	2.10	610	157	767	122	0.159

1.2. Surface area

Activated carbons are characterized by the presence of micropores of accessible widths L between 0.35 and 2 nm. Their volume W_o can be as high as 0.8 to 1 $cm^3\ g^{-1}$ and even more, which corresponds to 9-11 mmol of liquid-like benzene. A number of studies, for example [4,10,11], suggest that micropores are ideally slit-shaped, at least up to widths L and extensions of 1 to 1.2 nm. This structure is due to the presence of aromatic (or graphitic) sheets, reminiscent of the structure of non-porous carbon blacks. Larger micropores, sometimes called supermicropores, have more complicated and cage-like structures [11]. A possible model [12] is shown in Fig. 1.

Figure 1. Possible model for the structure of activated carbons, where the micropores correspond to slits between locally parallel aromatic sheets (reprinted from [1,12]).

In view of the small dimensions involved, the surface area of the micropore walls, S_{mi}, can be as high as 1500 to 1700 $m^2\ g^{-1}$. A reliable assessment of this area is provided by the simple geometrical relation valid for open slits of average width L_o,

$$S_{mi}\ (m^2\ g^{-1}) = 2000\ W_o\ (cm^3\ g^{-1})/L_o\ (nm) \qquad (1)$$

As discussed in detail elsewhere [6, 13], areas above 1500 to 1700 $m^2\ g^{-1}$, mainly based on the so-called BET technique are often unrealistic, since a single sheet of carbon has a total area of 3000 $m^2\ g^{-1}$ and carbons contain at least 2 to 3 graphitic layers.

The real surface area of microporous carbons can be assessed by independent techniques discussed below, such as the selective adsorption, from aqueous solutions, of sparingly soluble organics such as caffeine and phenol [7,8], comparison plots [14] and the modelling of vapour adsorption [15].

Beside micropores, activated carbons may also present meso and macroporosity with relatively important volumes, but the corresponding surface areas S_e usually do not exceed 100 to 150 $m^2\ g^{-1}$. The total surface area is therefore

$$S_{tot} = S_{mi} + S_e \qquad (2)$$

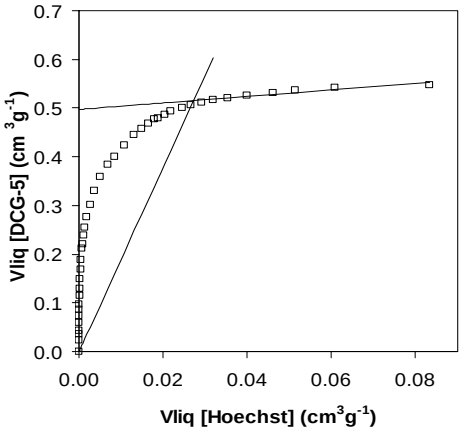

Figure 2. Comparison plot for the adsorption of benzene at 293 K on activated carbon DCG-5, the reference being graphitized carbon black *Hoechst.* The amounts adsorbed are expressed in cm^3 of liquid C_6H_6. The plot leads to a pore volume of 0.50 $cm^3\ g^{-1}$, S_{tot} = 1023 $m^2\ g^{-1}$ and S_e = 33 $m^2\ g^{-1}$, in good agreement with other techniques (see Table 1). The corresponding micropore distribution is shown in Figure 4.

Each contribution can be determined separately, for example with the help of a comparison plot. This technique, suggested originally by Sing [14], is based on the comparison of the nitrogen adsorption isotherm obtained at 77 K for an unknown sample and a non-porous reference such as *Vulcan-3G*. However, it is also possible to use benzene at room temperature, as illustrated in Fig. 2 for activated carbon DCG-5 and graphitized carbon black *Hoechst*.

The points of the graph correspond to the successive amounts adsorbed by both samples at the same absolute or relative pressures. As discussed by Kaneko *et al.* [16] and others [17], if the unknown carbon is not porous, the comparison plot leads to a straight line and its slope is proportional to the ratio of the two surfaces. The presence of microporosity is reflected by the upward deviation (loop), whereas the line through the origin should be close to the total surface area of the carbon.

The onset of the second linear section, at relative pressures beyond 0.4 to 0.6, depends on the filling of the smaller mesopores, if present. It is followed by adsorption on the walls of the larger pores and reflects the so-called external surface area S_e, which has properties similar to that of a non-porous carbon. The extrapolation of this linear section corresponds to V_p, the amount filling the micropores and the narrow mesopores.

The technique of the comparison plot can also be used to detect pores commonly found in templated carbons and probably intermediates between supermicropores and mesopores. This is illustrated in Figure 3, for templated carbon C-25-HT [13], using nitrogen adsorption at 77 K.

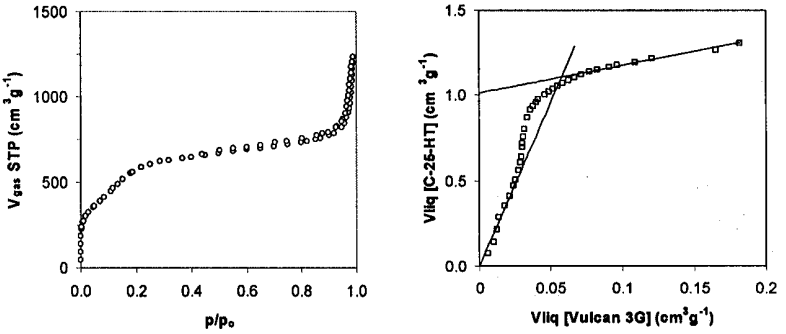

Figure 3. N_2 isotherm on templated carbon C-25-HT at 77 K (left) and comparison plot (right, reprinted from [13]) the reference being *Vulcan 3G*.V_p = 1.0 cm^3 g^{-1}, S_{tot} = 1546 m^2 g^{-1} and S_e = 133 m^2 g^{-1}.

The nitrogen isotherm (left) displays a step around p/p_o = 0.2, but without hysteresis on desorption. This corresponds to the deviation from linearity observed in the comparison plot (right). Moreover, the comparison with Figure 2 indicates the absence of microporosity, since there is no deviation from linearity at an early stage. One may therefore conclude that this templated carbon, like many others, has only narrow mesopores, reflecting the structure of the parent compound. They may be defined as *sub-Kelvin* mesopores, since the Kelvin equation [14] does not apply (no capillary condensation occurs). In the present case, their volume V_p = 1.0 cm^3 g^{-1}.

Recently, it has also been shown that the surface area of the micropore walls can be determined by the adsorption, from aqueous solutions, of sparingly soluble organic such as caffeine and phenol [7,8].

It follows, that both the microporous and external surface areas of activated carbons can be determined with a reasonable accuracy, but the BET surface areas do not always agree with the other determinations. For example,

in the case of PX-21 a carbon with a specific capacitance of 322 F g^{-1} in the 2 M H_2SO_4 electrolyte, the real total surface area is around 1270 m^2 g^{-1}, against S_{BET} of 3210 m^2 g^{-1}. Obviously, this difference has implications on the determination of specific properties expressed in terms of unit surface, for example F m^{-2} in the case of electric double layer capacitances (in the present case, 0.253 F m^{-2} instead of 0.100 F m^{-2}).

As discussed elsewhere [6], it appears that $S_{BET} - S_e$ simply corresponds to the monolayer equivalent of W_o, 2200 m^2 cm^{-3} in the case of nitrogen at 77 K.

1.3. Micropore and mesopore size distributions

The micropore distribution of an activated carbon can be determined in different ways and the traditional approach is based on molecular-sieve effects. Industrially activated carbons have usually been subjected to degrees of burn-off (weight loss on activation) of at least 30 to 50% and show practically no 'gate' effects at the entrance of the pore system. It is therefore possible to assess its accessibility to vapour and/or liquid probes with critical molecular dimensions L_c between approximately 0.35 (nitrogen, argon) and 1.5 nm (Tri-2,4-xylyl phosphate).

In the case of vapour adsorption, the isotherms of nitrogen and/or benzene give information on the total micropore volume W_o and the average micropore width L_o. For larger molecular, the analysis of the isotherm leads to the volumes $W(L_c)$ filled by the different probes. From a set of molecules and the corresponding function $W(L_c)$, it is therefore possible to derive a histogram $\Delta W(L_c)/ \Delta L_c = f(L_c)$.

A complementary approach [4-6] is based on the enthalpy of immersion $\Delta_i H$ of the carbon into liquids with increasing dimensions L_c. This technique is faster than adsorption of vapours and allows the use of probes which may have vapour pressures too low to be used in classical gravimetric experiments. More recently, modelling based on the computer simulation of CO_2 adsorption, mainly at 273 K, has been used to derive micropore size distributions [18]. The approach rests on the analysis of the overall experimental isotherms with the help of model isotherms for slit-shaped micropores of widths between 0.4 and 2 nm. Fig. 4 shows the correlation obtained by both techniques in the case of carbon DCG-5, where L_o = 1.1 nm. Due to 'gate' effects in the lower part of the pore size distribution, even small liquid molecules cannot fill all the micropores below 0.6 to 0.8 nm, as opposed to CO_2 .

It must also be pointed out that the cumulative surface area of the slit-shaped micropores based on CO_2 modelling is in good agreement with that obtained by other techniques such as comparison plots and the selective adsorption of phenol or caffeine from aqueous solutions.

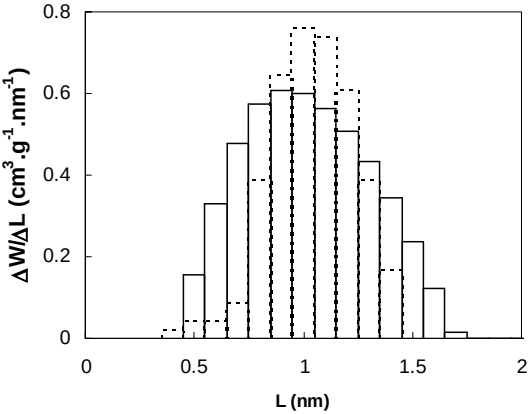

Figure 4. Pore size distribution of activated carbon DCG-5 obtained from immersion calorimetry (--) and from the CO_2 (273 K) adsorption isotherm (—) (reprinted from [6]).

Mesoporosity in carbons can be assessed by standard techniques based on the analysis of the hysteresis loop of the nitrogen or benzene isotherm [14, 20], which results from capillary condensation in pores with radii or widths above 2 nm. This analysis leads to the pore size distribution and their cumulative surface area. In principle, the latter is close to S_e, the surface area found outside the micropores.

1.4. Accessibility of the micropores to classical electrolytes

An important point raised in electrochemistry is the accessibility of the micropores to the various types of aprotic and organic electrolytes. It has often been argued that a large proportion of the micropores were not accessible even to the small inorganic electrolytes. However, the solvated SO_4^{2-} ion has a size of 0.53 nm [21], which means that practically the entire micropore system of the carbons listed in Table 1, should be accessible to it. This is also suggested by the comparison of the enthalpies of immersion of carbons containing only small amounts of oxygen (to avoid reaction with basic groups) into the electrolyte solution and into benzene. Consequently, for industrial carbons with pore sizes above 0.7 nm, the total surface area is accessible and may be taken into account for the evaluation of specific EDLC properties.

In the case of aprotic electrolytes such as $(C_2H_5)_4NBF_4$ in acetonitrile the accessibility can be tested with the help of the enthalpies of immersion of the carbons into the electrolyte and into benzene. As shown in Fig. 5, for typical carbons with L_o between 0.8 to 0.9 nm and 2 nm there exists a linear correlation between the two enthalpies, which suggests the same degree of accessibility.

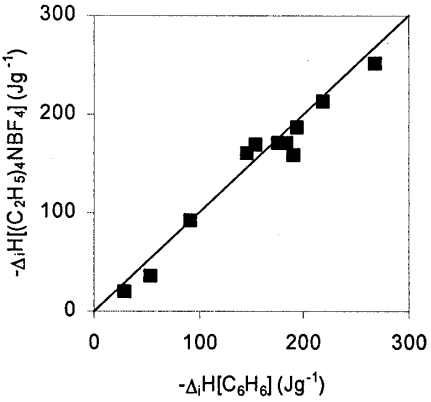

Figure 5. Correlation between the enthalpy of immersion of active carbons into 1M $(C_2H_5)_4NBF_4$ in acetonitrile, $-\Delta_i H((C_2H_5)_4NBF_4)$ and into benzene, $-\Delta_i H(C_6H_6)$ at 293 K.

Although the micropores are accessible to the individual molecules, it is likely that limitations may arise within pores below 0.8 to 1 nm (see Fig. 4). In this confined environment two layers cannot be formed completely by adsorption on the opposite walls and three dimensional clusters may be limited in size, at least in one direction.

By analogy with kinetic and self-diffusion effects observed in vapour adsorption, one may also expect that, in the case of supercapacitors, ionic mobility is reduced in small pores. This has implication on electrochemical properties in rapidly varying fields, as well as in the release of stored energy. These structural limitations must be added to chemical barriers such as carboxylic groups, found in the entire microporous structure and discussed below.

2. Chemical groups and their distribution in the micropores

As discussed by different authors, and in particular Figueiredo *et al.* [22], untreated and treated activated carbons contain, apart from hydrogen, a variety of chemical species such as carboxylic, lactonic, phenolic and quinonic groups. They can be titrated by classical techniques, such as Boehm's method [23] or immersion calorimetry into standard HCl, $NaHCO_3$ and NaOH solutions [24]. Thermally programmed desorption (TPD) [8,9,22,25] also provides useful information on the surface complexes and a satisfactory agreement has been found between the different techniques. The data obtained for both standard

and treated carbons of the present series, including graphite HSAG-300, is shown in Table 2.

Table 2. Amounts of CO and CO_2 determined by TPD.

Carbon	[CO] (meq g^{-1})	[CO_2] (meq g^{-1})
CMS	0.97	0.17
XC-72	$2 \cdot 10^{-4}$	0.01
AZ46-0	0.33	0.24
DCG-5	0.50	0.34
BV46	0.22	0.10
BV46-ox	2.01	0.63
PC-94-11-ox	1.20	0.86
SUPRA DLC-50	0.62	0.18
UO3	0.44	0.12
UO3-ox	1.42	0.88
(PX-21)	3.30	1.40
H25-ox	1.10	0.83
N-125	0.96	0.27
HSAG-300	0.65	0.38

Carbon itself is hydrophobic, but water interacts strongly with oxygen-containing surface groups and combined studies of immersion calorimetry and TPD [26] suggest an interaction energy of -10 J per mmol of oxygen. Consequently, one may expect that in the case of aqueous electrolytes the strong affinity of water for the surface groups and the formation of clusters also play an important role.

It has been argued that surface groups are found mainly on the external surface area [27], but there is evidence that they are distributed over the entire micropore system. This is suggested by a technique based on the determination of the enthalpy of immersion of the carbon into water, following the preadsorption of n-undecane [28]. For example, in the case of carbon U03-ox, one finds that the specific enthalpy of immersion $\Delta_i H(H_2O)/S_{tot}$ decreases from -0.083 J m^{-2} (no preadsorption) to -0.042 J m^{-2} for the external surface (all pores filled). For comparison, the limiting value for carbons without oxygen should be -0.030 J m^{-2}. More recently, computer modelling of water adsorption [29] confirmed the presence of oxygen over the entire microporous structure.

It follows that the presence of oxygen-containing groups over the entire microporous structure increases the complexity of the problem, since it must be added to the purely structural constraints imposed by the pore size distribution and the connectivity of the pores.

3. Electrochemical properties of carbons in relation to their structural and chemical characteristics

The foregoing sections illustrate the need for a good understanding of the structural and chemical aspects of activated carbons, in order to obtain reliable correlations. With respect to earlier studies of electrochemical properties, it appears that

(a) The total surface area based on the BET approach may be misleading, especially beyond 1500 $m^2 g^{-1}$ and may imply incorrect numerical values, for example specific capacitance given in F m^{-2}.
(b) For typical activated carbons with average micropore widths L_o above 0.8 to 1 nm, the structure should be accessible to classical electrolyte. However, problems may arise as far as the formation of clusters is concerned, due to the confined space. In narrow pores mobility will be reduced.
(c) Oxygen-containing species are distributed throughout the micropore system.

These observations may provide the basis for an improved description of electrochemical performance, as discussed below.

3.1 Experimental details on electrochemical measurements

The present study deals mainly with the specific capacitance of a series of activated carbons, used in work by the present authors, as well as data taken from the recent literature.

The electrochemical measurements were carried out in an *Autolab-Ecochimie PGSTAT30* potentiostat-galvanostat. Sandwich-type capacitors were prepared with two carbon pellets (8 mm in diameter) separated by glassy fibrous paper and placed inside a Swagelok-cell. The electrodes (11-12 mg) were obtained by pressing a mixture of 75 wt% of carbon, 20 wt% of polyvinylidene fluoride and 5 wt% of carbon black (Super P). 2M H_2SO_4 aqueous solution was used as electrolyte.

The capacitance C was determined by galvanostatic charge-discharge voltage cycles from 0 to 0.8 V at current density *d* between 1 and 150 mA per cm^2 of electrode surface. Reliable measurements were taken after 40 preliminary cycles. The specific capacitance C (Fg^{-1}) of a single electrode has been calculated by using the expression

$$C = 2\, I\, (\Delta t_d)/(m_c\, \Delta V_d) \qquad (3)$$

where I is the current, Δt_d is the time spent during the discharge, ΔV_d is the voltage decrease in the discharge and m_c the weight of carbon loaded in the composite electrode [2]. From this data, it is possible to calculate the capacitances in F per gram for the actual capacitor (carbon + carbon black + binder, etc.). Cyclic voltammetry experiments at scan rates of 1, 2, 5, 10, 20 and 50 mV s^{-1} were also used for estimating the specific capacitance of each electrode.

A satisfactory agreement was found between both techniques. Furthermore, preliminary tests with a three-electrode cell [1] for a selection of carbons of the present series (Courtesy Dr. M. Hahn, *Paul Scherrer Institute Villigen*, Switzerland), provided comparable results.

In the present work, our correlations are based exclusively on the galvanostatic charge-discharge cycles on two-electrode system.

The energy density (E) was deduced as $(1/2)C_c(\Delta V_d)^2$, C_c being the capacitance of the two-electrode capacitor cell, whereas the power was estimated from $E/\Delta t_d$. Both parameters are relative to the carbon mass in capacitor cell.

3.2. Limiting capacitance C_o and structural and chemical properties of the carbons

A reasonable starting point is the study of C_o, the limiting capacitance at low current density *d*, by convention at 1 mA cm^{-2}. This property has been investigated by Shi [27] for more than 30 carbons (activated microbeads and fibers), using a 5 M KOH electrolyte. It was shown that for these well activated carbons S_{BET} is often larger than $S_{mi} + S_e$, which is not surprising (see section 1.2). These different areas were obtained respectively from the analysis of the nitrogen isotherm with the BET model, the DFT technique and comparison plots. Shi's data for C_o expressed in F m^{-2} and given by the ratio

$$C_o\,(F\ m^{-2}) = C_o\,(F\ g^{-1}) / S_{BET}\,(m^2\ g^{-1}) \qquad (4)$$

varies between 0.06 and 0.22 F m^{-2}. On the other hand, the data of Kierzek *et al.* [30] obtained for highly activated carbon fibers with S_{BET} of 2700 to 3200 $m^2\ g^{-1}$ and 1 M H_2SO_4 electrolyte, leads to values as low as 0.07 Fm^{-2}. One may conclude that the actual surface area is probably smaller than S_{BET}.

Since S_{BET} is often unreliable for carbons with high surface areas, it is not surprising that a better correlation can be obtained for C_o if one uses $S_{tot} = S_{mi} + S_e$. Shi's data leads to an average capacitance of (0.138 ± 0.038) F m^{-2} (standard deviation for 30 values). In the case of a series of carbons investigated by the present authors and based on 2 M H_2SO_4 [31], S_{tot} leads to (0.172 ± 0.038) F m^{-2}. The recent data of Gryglewicz *et al.* [32] for 1 M H_2SO_4 and 6 M KOH electrolytes leads respectively to (0.127 ± 0.028) F m^{-2} and

(0.095 ± 0.024) F m^{-2}. These sets of data show some similarities, but in view of their scatter, they are only indicative for industrial activated carbons and cannot be used for reliable predictions of C_o.

Such examples suggested that more refined approaches were needed, in order to obtain a better overall agreement between the different sets of experiments. It was first suggested by Shi [27] that C_o consists of separate contribution from S_{mi} and S_e,

$$C_o[F\ g^{-1}] = c_{mi}S_{mi} + c_{ext}S_{ext} \quad (5)$$

For his data, parameters c_{mi} and c_{ext} are respectively 0.195 and 0.74 F m^{-2} for activated microbeads and 0.145 and 0.075 F m^{-2} for activated fibers. Eqn. (5) provides a better description for C_o than the use of S_{BET} or S_{tot} alone, but the sets of c_{mi} and c_{ext} values quoted in the literature seem to differ between families of carbons. This means that a different approach must be found for a more general description, probably involving the chemistry of the surface.

An interesting clue is provided by the recent work of Bleda-Martinez *et al*. [33] who investigated KOH-activated carbons with BET surface areas up to 3500 $m^2\ g^{-1}$. Although these areas may be questioned, it was shown that there exists a good linear correlation between C_o/S_{BET} and $[CO]/S_{BET}$, where [CO] represents the amount of CO obtained from TPD. This suggests that the CO-generating surface species contribute to the EDLC at low current density, probably as a pseudo-capacitance. Furthermore, a regression analysis taking into account the amount of CO_2 released in TPD, also given by these authors, shows that the contribution of the latter groups to C_o is small.

The role of surface groups is also suggested by the work of Okajima *et al.* [34] on the plasma treatment of the KF-1500 fiber monitored by TPD. Their study suggests an increase in the specific capacitance $C_o(F\ g^{-1})$, using a H_2SO_4 electrolyte, with the number of oxygenated functional groups. Similar results can be derived from the data of Hsieh and Teng [35], Nian and Teng [36] and Cheng and Teng [37]. The latter's work, based on the 3M KOH electrolyte, suggests 80 F per meq of desorbed CO.

An overall assessment for 47 carbons including our data and the data found in the literature for the H_2SO_4 electrolyte [33, 35, 36] leads to

$$C_o\,(Fg^{-1}) = (0.081 \pm 0.007)\,(Fm^{-2})S_{tot}\,(m^2g^{-1}) + (63 \pm 5)(F\ meq^{-1})[CO](meq\ g^{-1}) \quad (6)$$

As illustrated by Fig. 6 one obtains an interesting pattern, but there are exceptions, as observed for certain samples strongly oxidized with $(NH_4)_2S_2O_8$ and where the contribution to the pseudo-capacitance is well below 63 F meq^{-1}. Such exceptions require a detailed study of the CO-generating surface complexes formed by this agent.

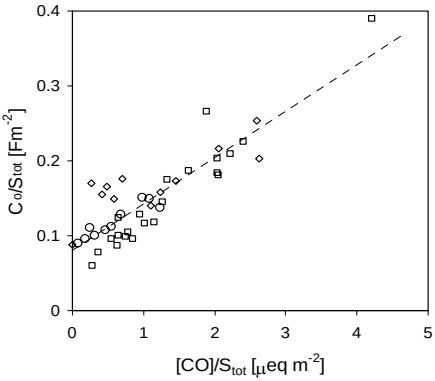

Figure 6. Correlation between C_o/S_{tot} and $[CO]/S_{tot}$ for the carbons of Table 2 (◊) and from refs. [33] (□) and [35,36] (○).

It is also interesting to point out that the average specific contribution of the total surface area alone (0.081 F m^{-2}) is close to the value of 0.088 F m^{-2} obtained for carbon XC-72, which contains only 0.01 meq of oxygen per gram (Table 2).

At this stage, it appears that Eqn. (6) may be regarded as an alternative to Eqn. (5), the expression proposed by Shi [27]. Instead of variable contributions from the microporous and external surface areas, C_o seems to depend on standard contributions from S_{tot} and the CO-generating groups, with the reservation expressed above regarding certain types of oxidation. Obviously, there may be numerical changes to Eqn. (6) in the light of new data, but it appears that the chemical nature of the surface plays a relatively important role in the capacitance at low current density. Eqn. (6) also applies to a wide range of activated carbons, whereas Eqn. (5) leads to different sets of parameters c_{mi} and c_{ext}, depending on the origin of the solids.

There is little doubt about the contribution of certain oxygen-containing groups to C_o, and it appears that other atoms may also play a role, which confirms possible contributions of chemical species to C_o. As shown recently by Kodama *et al.* [38] and by Frackowiak *et al.* [39], the presence of residual nitrogen from the precursor in the surface structure can increase considerably the specific capacitance of the carbon in the H_2SO_4 electrolyte. Obviously, this avenue should be investigated, in particular if the performance/cost ratio is favourable.

It is interesting to note that the surface groups which generate CO in TPD and contribute significantly to C_o occupy only a small fraction of the total surface area of the carbons. This surface area is part of the accessible edges or

indentations created by a strong chemical treatment (KOH). It corresponds to the so-called active surface area (ASA), a concept used some years ago by Ehrburger *et al.* [40,41]. Assuming, a molecular surface area of 0.083 nm^2 per desorbed CO molecule, or 50 m^2 per meq, the contribution of the corresponding groups to the capacitance is approximately 63 (F meq^{-1})/50(m^2 meq^{-1}) = 1.2 F m^{-2}. It follows that the average capacitance of 0.14 F m^{-2} obtained by Centeno *et al.* [13] for the external surface of typical carbons corresponds approximately to (0.140-0.081)/1.2 = 0.05 or 5% of the surface. In the case of the internal surface area S_{mi}, a similar calculation suggests 15% for the micropore walls of KOH-activated carbon PX-21. This is the direct result of KOH activation, which exposes existing edges or creates edges by an attack perpendicular to the basal planes [42, 43]. According to Y.J. Kim *et al.* [43], the edges represent approximately 7% in activated carbons, whereas C.H. Kim *et al.* [44] report values as high as 23%. However, edges and indentations may also contain [CO_2]-desorbing groups, which means that the real surface of the exposed edges is approximately one third higher for typical carbons since [CO]/([CO] + [CO_2]) is often around 0.7 to 0.8 (0.7 for the carbons of Table 2).

It is also interesting to point out that, as shown by Ehrburger *et al.* [41], the active surface area of various oxidized carbons, and consequently, the amount CO-generating surface groups attached to it, tends to increase with their micropore volume, W_o. His data suggests an upper bound

$$ASA(m^2\ g^{-1}) = 166(m^2\ cm^{-3})W_o(cm^3\ g^{-1}) \quad (7)$$

This correlation explains the empirical contribution of approximately 160 F cm^{-3} suggested earlier [31] for the best cases, to be added to Shi's Eqn. (5) and reflecting, effectively, the role of the CO-generating groups.

3.3. Variation of the specific capacitance with the current density

A first inspection of the cyclic voltammograms for different activated carbons indicates that the performance varies significantly from carbon to carbon.

As an example, the Supra DLC-50 capacitor shows a quick charge propagation revealed by the regular box-like shape of voltammograms preserved up to a scan rate of 50 mV s^{-1}. As shown in Fig. 7, the specific capacitance achieves a similar value over the whole range of sweep rates. The steep current change at the switching potentials reflects the major role of an accessible porous structure, which allows a rapid diffusion of ions.

By contrast, carbon PX-21 delivers a much higher specific capacitance at 2 mV s^{-1}, but it shows a deformed cyclic voltammogram at a scan rate of

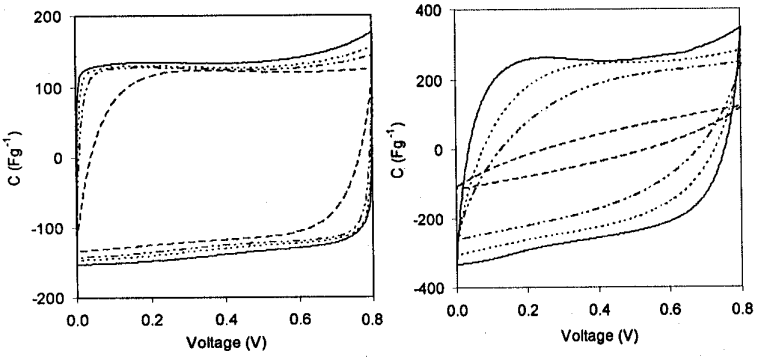

Figure 7. Cyclic voltammograms at different scan rates for carbons Supra DLC-50 (left) and (PX-21) (right). [2 mV s^{-1} (—), 5 mV s^{-1} (-----), 10 mV s^{-1} (— --), 50 mV s^{-1} (— —)].

10 mV s^{-1} and a completely collapsed one at 20 mV s^{-1}. This evolution indicates an increase in the ESR (equivalent series resistance) of the electrode due to the hindered motion of the charges in the porous network [2].

The different behaviour of active carbons in supercapacitors is confirmed by the galvanostatic charge-discharge profiles recorded at high current load (Fig. 8). It is well known that the specific capacitance, C, generally decreases when the current density, *d*, increases, typically up to 150-200 mA cm^{-2}.

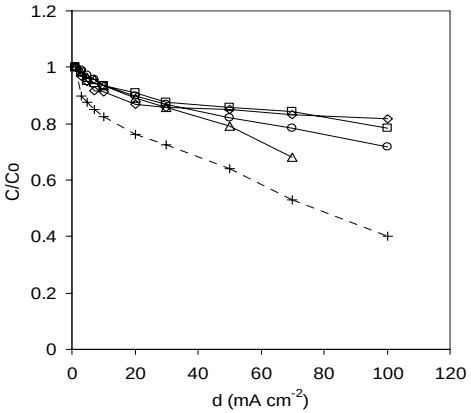

Figure 8. Variation of the relative capacitance C/C_o with the current density *d* for carbons Supra DLC-50 (◊), BV46 (□), CMS (○), UO3 (Δ) and PX-21 (+).

It has been suggested by different authors that oxygen-containing surface groups-in particular acids-may reduce the mobility of ions [35,36,45,46]. This means that the variation of C with *d* should also depend on [CO_2], the amount of CO_2 released by TPD and/or the milliequivalents of NaOH needed to titrate the acid groups. However, one may also expect that the mobility in the micropore system also depends, to some extent, on the average pore width L_o. By analogy with diffusion effects observed in the case of vapour adsorption, the influence of L_o should be added to the barriers created by the surface oxygen, which is present in the entire micropore system.

The analysis of the data for the 14 carbons of Table 2 and current densities *d* up to 150 mA cm^{-2} suggests that

$$C\ [F\ g^{-1}] = C_o \exp[\ -d\ (\ 0.00173/L_o + \ \ 0.00610\ [CO_2\ ])\ ] \qquad (8)$$

The correlation coefficient is 0.987 (150 experimental points and deviations mostly below 10 to 15 per cent). Larger deviations, observed mainly for strongly oxidized carbons beyond 100 to 150 mA cm^{-2}, may reflect factors not considered in Eqn. (8).

Taking also into account the corresponding amounts of CO in Eqn. (8) leads to -0.0004[CO]. This suggests that the variation of C with *d*, does not depend significantly on the CO-generating groups. On the other hand, the influence of $1/L_o$ on C is clearly suggested by carbons CMS, BV46, U03, Supra DLC-50 and XC-72 with relatively low [CO_2] contents and L_o between 0.75 and 1.8 nm. In this case, the leading term in the exponent of Eqn. (8) is $0.0019/L_o$, which appears to be 1.5 to 3 times larger than the contribution from the second term, 0.0069[CO_2], depending on the carbon.

The CO_2-generating surface species are mainly acidic groups and [CO_2] is often close to the meq of NaOH required to neutralize these groups. Therefore, it is not too surprising to obtain a correlation similar to Eqn. (8).

3.4. Physico-chemical properties of carbons and Ragone-type plots

The correlation of the physico-chemical properties of carbons with dynamic aspects such as the release of the stored electric energy is highly relevant to determine the potential application of different carbons in supercapacitors. As an example, Ragone-type plots relating power-density to achievable energy-density have been used in Fig. 9 for comparative evaluation of active carbons with a micropore size around 2 nm, such as N-125, H25-ox and PX-21. It should be pointed out that the supercapacitor performance is not limited by the carbons themselves, but it also depends on the experimental device. Figure 9 provides quite reliable information on the relative potential performance of the carbons as far as all samples were tested under the same

experimental conditions. It is likely that the performance is improved by using a commercial set up.

As expected from their similar specific surface areas and not very different content in [CO]-desorbing groups, the capacitors from carbons N-125 and H25-ox provide a similar energy density (about 3 Wh kg^{-1} with a cell voltage of 0.8 V) at low current density. However, the device based on H25-ox delivers only 513 W kg^{-1} at about 0.7 Wh kg^{-1} whereas the capacitor from N-125 can reach 1417 W kg^{-1}. On the other hand, it must be pointed out that the profile for Energy-Power dependence for the latter is very similar to that found for the non-porous graphite HSAG-300 with relatively low [CO_2] content. The lower rate for energy delivering of carbon H25-ox may be ascribed to the 3 times higher amount of [CO_2]-surface groups than for carbon N-125 (Table 2). With carbon PX-21 one obtains a quite different behaviour. Its high surface area and high content of [CO]-generating groups allow this material to store energy as high as 7 Wh kg^{-1} at low discharge rate. However, this carbon is not a good option, since for high power applications the energy density drops with increasing power output (Fig. 9). It is believed that the transport of solvated ions during the charge-discharge process is hindered by its high content in [CO_2]-generating groups. The increasing internal pore resistance leads to a non-uniform power capability [2].

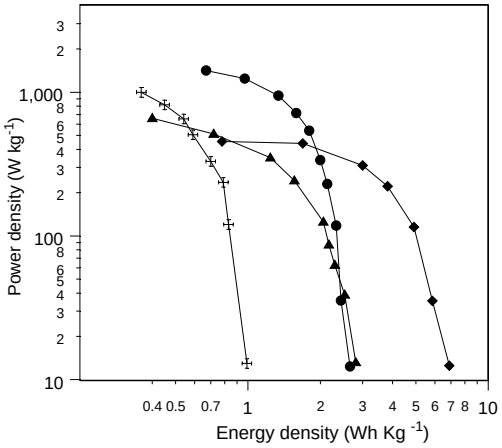

Figure 9. Power density *vs.* Energy density for activated carbons with a micropore size around 2 nm. N-125 (●), H25-ox (▲), PX-21 (♦). Non-porous graphite HSAG-300 (+) is included for comparison. The data was obtained under similar experimental conditions.

Unfortunately, there are exceptions and it is not possible, at this stage, to explain the performance of all carbons on the basis of this approach. For example, carbons BV-46-ox and UO3-ox, which have been oxidized under conditions different from those taking place under standard steam or CO_2 activation. As a result, the nature of the oxygen-containing groups may be rather different. Further studies should consider in more detail the effect of the different surface groups on the performance of carbons in electrochemical capacitors.

On the other hand, one must take into account that electronic conductivity, affinity to electrolytic solution, wettability, hydrophobic/hydrophilic character and other intrinsic properties of electrodes also play a key role on the performance of carbons in supercapacitors.

4. Conclusions

This paper shows that the assessment of carbons to be used as supercapacitors requires a reliable structural and chemical characterization. In the present case, the use of this information is limited to the study of the electric double layer capacitance determined with the 2 M H_2SO_4 electrolyte, but it appears that this approach provides a better overall picture. The relevant features examined here are:

(a) The BET surface area is often unreliable for carbons with high surface areas, which are precisely the most interesting candidates as supercapacitors. This leads to contradictory results for the specific capacity given in F m^{-2}.

(b) As suggested by immersion calorimetry, the accessibility of the micropore system of typical activated carbons to aprotic electrolytes is similar to that of benzene, a reference molecule used for the structural characterization of these solids. To some extent, the same applies to the classical organic electrolytes such as $(C_2H_5)_4NBF_4$ in acetonitrile used with carbons where L_o is above 0.8-1 nm.

(c) The capacitance at low current density, C_o, depends on the total surface area and on the surface groups which generate CO in TPD. The contribution from the latter corresponds to a pseudo-capacitance. Eqn. (6) replaces the earlier correlation suggested by Shi [27], which considers different contributions from S_{mi} and S_e, but does not lead to an overall agreement between different classes of carbons.

(d) Oxygen-containing groups are distributed over the entire micropore system and not limited to the external surface area, as shown by immersion calorimetry and confirmed by the modelling of water adsorption isotherms in various pore size distributions. This means that the entire micropore system and the oxygen contained in it contribute to the electrochemical properties. Moreover, in the case of the variation of C with the current density *d*, given by

Eqn. (8), it appears that both the CO_2-generating surface groups and the average micropore width L_o play a role. The influence of $1/L_o$ is perceptible for activated carbons with low oxygen contents, but for oxidized carbons the CO_2-generating groups (acids) have a predominant effect on the capacitance.

Obviously, the elements presented here are only the first stage of an attempt to provide a better understanding of the relation between the structural and the chemical characteristics of activated carbons, on the one hand, and some of their properties when used as supercapacitors. Further steps should consider in more detail the correlation with dynamic aspects such as the release of stored electric energy and electrochemical properties at high frequencies.

Acknowledgements

The authors wish to thank Dr. M.J. Lázaro (Instituto de Carboquímica-CSIC) for TPD experiments and Dr. M. Hahn (PSI Villigen, Switzerland) for useful discussions.

References

1. Bansal, R.C., Donnet, J.B. and Stoeckli, F. 1988, Active Carbon, Marcel Dekker, New York, 1-26, 119-162
2. Conway, B.E. 1999, Electrochemical Supercapacitors, Kluwer Academic, New York, 183.
3. Stoeckli, F. 1990, Carbon, 28, 1.
4. Stoeckli., F. 1995, Porosity in carbons-characterization and applications, J. Patrick (Ed.), Arnold, London, 67.
5. Stoeckli, F. and Centeno, T.A. 1997, Carbon, 35, 1097.
6. Stoeckli, F. and Centeno, T.A. 2005, Carbon, 43, 1184.
7. Fernández, E., Hugi-Cleary, D., López-Ramón, M.V., and Stoeckli, F. 2003, Langmuir, 19, 9719.
8. López-Ramón, M.V., Stoeckli, F., Moreno-Castilla, C. and Carrasco-Marín, F. 2000, Langmuir, 16, 5967.
9. Carrasco-Marín, F., Mueden, A., Centeno, T.A., Stoeckli, F., and Moreno-Castilla, C. 1997, J. Chem. Soc. Faraday Trans., 93, 2211.
10. Fryer, J.R. 1981, Carbon, 19, 431.
11. Marsh, H, Crawford, D. O'Grady, T.M., and Wennerberg, A. 1982, Carbon, 20, 419.
12. Stoeckli, F., Kraehenbuehl, F., Lavanchy, A., and Huber, U. 1984, J. Chim. Physique, 81, 785.
13. Centeno, T.A., Sevilla, M., Fuertes, A.B., and Stoeckli, F. 2005, Carbon, 43, 3012.
14. Gregg S.J., and Sing, K,S,W. 1982, Adsorption, Surface Area and Porosity, Academic Press, New York, 94.
15. Stoeckli, F., Guillot, A., Slasli, A., and Hugi-Cleary, D. 2002, Carbon, 40, 383.
16. Kaneko, K., Ishii. C., Ruike. M., and Kuwabara. H. 1992, Carbon, 30, 1075.
17. Setoyama, N., Suzuki, T., and Kaneko, K. 1998, Carbon, 36, 1459.

18. Stoeckli, F., Slasli, A., Hugi-Cleary, D., and Guillot, A. 2002, Microp. Mesop. Mater., 51, 197.
19. Slasli, A.M., Jorge, M., Stoeckli, F., and Seaton, N.A. 2003, Carbon, 41, 479.
20. Stoeckli, F., Kraehenbuehl, F. 1984, Carbon 22, 297.
21. Endo, M., Maeda, T., Takeda, T., Kim, Y.J., Koshiba, K., Hara, H., and Dresselhaus, M.S. 2001, J. Electrochem. Soc., 148, A910.
22. Figueiredo, J.L., Pereira, M.F.R., Freitas, M.M.A., and Orfao, J.J.M. 1999, Carbon, 37, 1379.
23. Boehm, H.P.1966, Advances in Catalysis, D. Eley, H. Pines, P.B. Weisz (Eds.), Academic Press, New York, 179.
24. Lopez-Ramón, M.V., Stoeckli, F., Moreno-Castilla, C. and Carrasco-Marin, F. 1999, Carbon, 37,1215.
25. Haydar, S., Moreno-Castilla, C., Ferro-García, M.A., Carrasco-Marín, F., Rivera-Utrilla, J., Perrard, A., and Joly, J.P. 2000, Carbon, 38, 1297.
26. Stoeckli, F. and Lavanchy, A. 1999, Carbon, 37, 315.
27. Shi, H. 1996, Electrochim. Acta, 41, 1633.
28. Stoeckli, F., Huguenin, D., Rebstein, P. 1991, J. Chem. Soc. Faraday Trans., 87, 1233.
29. Slasli, A.M., Jorge, M., Stoeckli, F., and Seaton, N.A. 2004, Carbon, 42, 1947.
30. Kierzek, K., Frackowiak, E., Lota, G., Gryglewicz, G., and Machnikowski, J. 2004, Electrochim. Acta, 49, 515.
31. Centeno, T.A., and Stoeckli, F. 2006, J. Power Sources, 154, 314.
32. Gryglewicz, G., Machinowski, J., Lorenc-Grabowska, E., Lota, G., Frackowiak, E. 2005, Electrochim. Acta, 50, 1197.
33. Bleda-Martínez, M.J., Maciá-Agulló, J.A., Lozano-Castelló, D., Morallón, E., Cazorla-Amorós, D., Linares-Solano, A. 2005, Carbon, 43, 2677.
34. Okajima, K., Ohta, K., Sudoh, M. 2005, Electrochim. Acta, 50, 2227.
35. Hsieh, C.T., and Teng, H. 2002, Carbon, 40, 667.
36. Nian, Y.R., and Teng, H. 2003, J. Electroanal. Chem., 540, 119.
37. Cheng P.Z., and Teng, H. 2003, Carbon, 41, 2057.
38. Kodama, M., Yamashita, J., Soneda, Y., Hatori, H., Nishimura, S., and Kamegawa, K. 2004, Mat. Sci. Eng. B, 108, 156.
39. Frackowiak, E., Lota, G., Machnikowski, J., Vix-Guterl, C. and Béguin, F. 2006, Electrochim. Acta, 51, 2209.
40. Ehrburger, P., Louys, F, and Lahaye, J. 1989, Carbon, 27, 389.
41. Ehrburger, P., Pusset, N., Dziedzinl, P. 1992, Carbon, 30, 1105.
42. Endo, M., Lee, B.J., Kim., Y.A., Kim, Y.J., Muramatsu, H., Yanagisawa, T., Hayashi, T., Terrones, M., and Dresselhaus, M.S. 2003, New Journal of Physics, 5,121.1.
43. Kim, Y.J., Horie, Y., Matsuzawa, Y., Ozaki, S., Endo, M., and Dresselhaus, M. 2004, Carbon, 42, 2423.
44. Kim, C.H., Pyun, S.I., and Kim, J.H. 2003, Electrochim. Acta, 48, 3455.
45. Nakamura, M., Nakanishi, M.,Yamamoto, K. 1996, J. Power Sources, 60, 225.
46. Kim, C.H., Pyun, S.I., Shin, H.C. 2002, J. Electrochem. Soc., 149, A93.